Available online at website: https://journal.bcrec.id/index.php/bcrec

Bulletin of Chemical Reaction Engineering & Catalysis, 21 (3) 2026, 749-759

Original Research Article

Green Synthesis of Silver Nanoparticles Using Soursop Leaf Extract for Photocatalytic Degradation of Textile Wastewater

Iryanti Eka Suprihatin[1*], Anak Agung Sagung Alit Sukmaningsih[2], Ni Made Utami Dwipayanti[3], Ida Ayu Gede Widihati[1], Ni Putu Diantariani[1], Ni Gusti Ayu Dwi Adhi Suastuti[1], I Gusti Ayu Kunti Sri Panca Dewi[1]

[1]*Department of Chemistry, Faculty of Mathematics and Natural Sciences, Universitas Udayana, Jl. Raya Kampus UNUD, Bali, 80361, Indonesia.*
[2]*Department of Biology, Faculty of Mathematics and Natural Sciences, Universitas Udayana, Jl. Raya Kampus UNUD, Bali, 80361, Indonesia.*
[3]*Department of environmental science, Postgraduate Building, Universitas Udayana, Jl. P.B. Sudirman, Denpasar, Bali, 80114, Indonesia.*

Received: 8th May 2026; Revised: 4th July 2026; Accepted: 4th July 2026
Available online: 13th July 2026; Published regularly: October 2026

Abstract

This study aimed to synthesize silver nanoparticles (AgNPs) as a photocatalyst and evaluate their performance for textile wastewater photodegradation since previous studies have mainly focused on photocatalytic degradation of model dye compounds, whereas studies using actual textile wastewater remain limited. The synthesis was achieved by extracting soursop leaves and mixing them with $AgNO_3$ and heating the mixture. After photodegradation reaction condition optimization, the optimum conditions were found at pH of 13, 15 minutes of irradiation time, and a volume of 0.5 mL of AgNPs. Under these conditions, a degradation percentage of 34.37-37.76% was achieved, with a reduction in BOD levels of 5.54-11.08% and COD levels of 8.66-12.22%. These results indicate the potential of AgNPs for textile wastewater treatment, although pretreatment may be required to improve degradation performance.

Keywords: Dyes; Photocatalytic; Photodegradation; Silver nanoparticles; Soursop leaf extract; Textile wastewater

How to Cite: Suprihatin, I. E., Sukmaningsih, A. A. S. A., Dwipayanti, N. M. U., Widihati, I. A. G., Diantariani, N. P., Suastuti, N. G. A. D. A., Dewi, I. G. A. K. S. P. (2026). Green Synthesis of Silver Nanoparticles Using Soursop Leaf Extract for Photocatalytic Degradation of Textile Wastewater. *Bulletin of Chemical Reaction Engineering & Catalysis*, 21 (3), 749-759. (DOI: 10.9767/bcrec.20726)

Permalink/DOI: https://doi.org/10.9767/bcrec.20726

1. Introduction

As the textile industry develops rapidly in Indonesia, the presence of dye waste is increasing as well. The dye waste can cause dangerous pollution to aquatic environments, as it is stable, difficult to decompose, and toxic [1,2]. Local industries treat their textile waste using conventional processing methods such as bleaching and neutralization, followed by gravitational sedimentation. These conventional methods are not effective to remove the pollutants contained in the waste. This weakness necessitates the development of more effective and promising alternatives, such as biodegradation or photodegradation. Photocatalytic degradation is a cost-effective, environmentally friendly, and efficient method for removing waste that contains high concentrations of organic materials, such as textile dyeing waste. This process involves the formation of reactive radicals that can oxidize hazardous compounds contained in the waste. Therefore, photocatalytic degradation is currently a widely developed method [3,4].

Photocatalytic degradation is a mechanism for simplifying organic compounds by utilizing light energy, such as UV light and sunlight, with the aid of a catalyst [5]. Using visible light as an energy source in the photodegradation process offers the added advantage of directly harnessing

* Corresponding Authors.
Email: eka_suprihatin@unud.ac.id (I.E. Surpihatin)

solar energy, making the process more energy-efficient and sustainable [6,7]. Photocatalysts play a crucial role in the photodegradation process, necessitating the development of materials that can function as photocatalysts. These materials are typically those with an energy gap between the conduction band and the valence band, which can be overcome by photon energy in the range of ultraviolet (UV) or visible light, depending on the band gap of the material [8,9]. This gap provides potency for electrons on the valence band to excite to the conductance band when the material absorbs a photon. The electron excitation leaves a positive hole on the valence band and creates a negatively charged conductance band. These charges react with water or oxygen molecules in their environment, resulting in reactive radicals, which in turn react with organic materials in contact with them and thus degrade the materials into simpler molecules [10].

Semiconductors can act as photocatalysts. Metal conductors, on the other hand, having no energy gap, do not have the ability to provide radicals. However, by reducing the particle sizes of the metal, it can increase the energy gap [11], making it function as a photocatalyst. The smaller the size of the catalyst particles, the larger the surface area, allowing for more even distribution in the waste to be degraded [12]. Metal nanoparticles are metal-based materials with particle sizes less than 100 nm [13,14]. An example is silver nanoparticles (AgNPs). AgNPs is one of the most widely studied nanoparticles due to its non-toxic properties and excellent antibacterial properties against several microorganisms that can cause various diseases. AgNPs have benefits in many fields, including their ability to detect optical sensors and their use as a photocatalyst [15,16].

Metal nanoparticle synthesis typically uses a top-down (physical) or bottom-up (chemical) approach, but these methods have limitations such as the use of toxic solvents, production of toxic waste, and high energy consumption [17,18]. Therefore, phytosynthesis is often chosen for silver nanoparticle synthesis. Phytosynthesis is a nanomaterial synthesis process that involves plant extracts as reducing and stabilizing agents. Plant extracts contain bioactive compounds such as flavonoids, polyphenols, and alkaloids, which are able to reduce metal ions [19–21].

The soursop plant is widely known for its diverse benefits because almost every part of the plant can be utilized, including its leaves. This is because Soursop leaves (*Annona muricata*) contain various bioactive compounds, including alkaloids, terpenoids (steroids), tannins, coumarins, and flavonoids [5,22–24]. Soursop leaf extract contains various types of dihydroflavonols, flavonoids, flavonols, and flavones and flavanones, making it a promising candidate as a bioreductant in the synthesis of silver nanoparticles.

Several studies have demonstrated that silver nanoparticles (AgNPs) as photocatalysts can degrade dyes. According to Lestari *et al.* [25], under optimal conditions, 94.75% of indigosol blue dye can be degraded by AgNPs. These conditions include an irradiation time of 4 hours, a volume of 2 mL, and an acidity level of pH of 3. Research by Suprihatin *et al.* [5] successfully degraded 99% of 700 ppm Congo red and indigo carmine, respectively, using 1 and 5 mL of AgNPs synthesized from soursop leaf water extract at pH 2 and an irradiation time of 60 minutes.

Most previous studies have focused on the degradation of individual dye compounds under controlled conditions model dye compounds such as methylene blue, methyl orange, and rhodamine B under controlled experimental conditions [9,26,27]. However, textile dyeing wastewater consists of a far more complex matrix containing various organic and inorganic substances in addition to dyes, making its treatment more challenging and representative of real environmental conditions. Therefore, investigating the degradation of textile wastewater is essential to bridge this research gap. In response to this need, this study reports the photocatalytic degradation of textile dyeing wastewater under visible-light irradiation using silver nanoparticles as a photocatalyst. The novelty of this work lies in the application of silver nanoparticles for the treatment of real textile dyeing wastewater rather than model dye solutions, providing new insights into their photocatalytic performance under practical wastewater conditions.

2. Materials and Methods

2.1. Materials and Equipment

Soursop leaves were collected from Central Java, Indonesia, and textile wastewater from a dyeing industry was obtained from Banjar Akta, Gianyar, Bali, Indonesia. All chemicals used in this study were of analytical grade and purchased from Merck unless otherwise stated. The chemicals included silver nitrate ($AgNO_3$), manganese sulfate ($MnSO_4$), sulfuric acid (H_2SO_4), magnesium (Mg), potassium dichromate ($K_2Cr_2O_7$), sodium thiosulfate pentahydrate ($Na_2S_2O_3 \cdot 5H_2O$), magnesium sulfate ($MgSO_4$), calcium chloride ($CaCl_2$), ferric chloride ($FeCl_3$), silver sulfate (Ag_2SO_4), and sodium hydroxide (NaOH). Acetic acid (CH_3COOH, 98.5%), chloroform ($CHCl_3$, 99.8%), ammonium hydroxide (NH_4OH, 25%), and hydrochloric acid (HCl, 37%) were also used., Mayer's reagent, Wagner's reagent, Dragendorff's reagent, starch indicator, demineralized water, distilled water, and EM4 (PT Songgolangit Persada, Indonesia).

The instruments used were an analytical balance (Kern ABS 220-4N, Kern & Sohn, Germany), vortex mixer (VM1, Ratek, Australia), pH meter (smart sensor AS218), COD reactor (T-25, K-nai), centrifuge (Clements 2000, Clements, Australia), UV–Vis spectrophotometer (Shimadzu UV-2600, Shimadzu Corporation, Japan), particle size analyzer (Malvern, Zetasizer Pro Blue, Malvern Panalytical, UK) and raman spectrometer (Bruker BRAVO).

2.2. Preparation of Soursop Leaf Water Extract

A water extract of soursop leaves was prepared based on previous work, involving the heating of 20 grams of air-dried soursop leaf powder in 1000 mL of distilled water for 15 minutes at 60 °C. Subsequent to chilling, it was subjected to filtration with filter paper. The prepared soursop leaf extract was sampled for phytochemical contents of alkaloids, terpenoids, flavonoids, saponins, and tannins.

2.3. Silver Nanoparticle Synthesis

Silver nanoparticles (AgNPs) were synthesized through a green synthesis approach by reacting 0.001 M $AgNO_3$ with soursop leaf extract. A 9:1 volume ratio was used, where 90 mL of 0.001 M $AgNO_3$ solution was mixed with 10 mL of soursop leaf extract. The mixture was heated at 40°C and maintained for 60 min. Formation of AgNPs was initially indicated by a color change from pale yellow to reddish-brown due to the reduction of Ag^+ ions and nanoparticle formation. Following synthesis, the resulting AgNPs were used directly as a colloidal suspension without separation from the residual plant extract. Consequently, the suspension contained dispersed AgNPs together with extract-derived molecules that may act as capping and stabilizing agents. The synthesized AgNPs were characterized using particle size analysis (PSA) to determine particle size distribution and zeta potential.

2.4. Textile Waste Characterization

The wastewater sampled from the main effluent of an industrial textile dyeing process was analysed for its pH (SNI 06-6989.11-2004), BOD (SNI 6989.72-2009), COD (SNI 6989.02-2019), maximum wavelength (UV-Vis spectrophotometer), and its absorbance. This procedure was conducted to determine the initial values before the photocatalytic degradation.

2.5. Determination of the Optimum Condition for The Degradation

Photocatalytic degradation experiments were conducted under visible-light irradiation within the wavelength range of approximately 400–500 nm. However, detailed specifications of the irradiation source, including lamp model, power output, irradiation intensity, wavelength distribution, and photon flux, were not available and should be considered a limitation of the present study. For this research, the optimum condition is defined as the pH, the AgNPs volume, and the irradiation time which gives the maximum degradation percentage of 20 mL of the textile waste. The degradation percentage was calculated using equation (1):

$$\%D = \frac{A_0 - At}{A_0} . 100\% \quad (1)$$

wherein: A_0 represents initial absorbance and A_t final absorbance.

To determine the optimum pH, 8 mixtures containing 2 mL AgNPs and 20 mL of the wastewater sample were adjusted to pH of 2, 4, 6, 8, 10, 11, 12 and 13 by adding 0.1 M HCl or 0.1 M NaOH. The mixtures were then irradiated with visible light for 30 minutes as shown in Figure 1. After irradiation, the mixture was centrifuged at 3000 rpm for 30 minutes, and the supernatants were analyzed for their absorbances. The optimum amount of the AgNPs for the degradation was determined by irradiating 20 mL of the wastewater sample with visible light using a varied volume of AgNPs of 1, 2, 5, 10, 15, and 20 mL under the optimum pH for 30 minutes and measuring the degradation percentage based on the decreasing absorbances. Five varied irradiation times of 15, 30, 45, 60, and 90 minutes were applied to determine the optimum irradiation time. The experiment was conducted as above using the optimum AgNPs volume under the optimum pH.

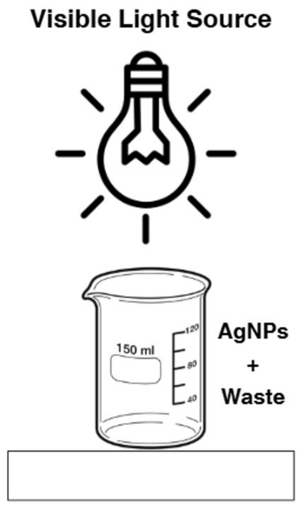

Figure 1. Illustration of wastewater sample photodegradation method using visible light and AgNPs.

2.6. Determination of the Effectiveness of the Photocatalytic Degradation of The Textile Dyeing Waste using AgNPs and Visible Light

The photocatalytic degradation effectiveness was determined by comparing the degradation percentages of the waste using AgNPs under optimum condition and without AgNPs. For this experiment, 500 mL of the textile wastewater was used for each analysis. The volume of the AgNPs was adjusted accordingly. The degradation percentage was calculated based on the difference in absorbance, BOD, and COD using equation (1), with "A" represents absorbance, BOD, or COD.

3. Results and Discussion

3.1. Phytochemical Screening

The phytochemical screening results indicated the presence of flavonoids, tannins, and terpenoids in the soursop leaf extract (Table 1), finding of which supports that reported by Suprihatin *et al.* [5]. This suggests that similar classes of phytochemicals are commonly present in Annona muricata leaves, although their composition and concentration may vary depending on environmental and geographical factors [28].

The presence of flavonoids, tannins, and terpenoids has been shown to act as bioreductive and stabilizing agents in the synthesis of silver nanoparticles (AgNPs). A study by Zuhrotun *et al.* explicitly demonstrated that the combination of flavonoids, tannins, and terpenoids is highly effective in producing stable silver nanoparticles [29]. This demonstrates the great potential of soursop leaves in nanoparticle synthesis, which is not only environmentally friendly but also chemically efficient.

3.2. Silver Nanoparticle Synthesis

A color change to reddish-brown indicates silver nanoparticles. The results of silver nanoparticle synthesis can be seen in Figure 2. The synthesis process utilizes soursop leaf extract, which contains secondary metabolites that act as bioreductants. The hydroxyl groups (-OH) in the terpenoids and tannins in the extract donate electrons to Ag^+ ions, reducing them to Ag atoms and producing AgNPs [30]. The formation mechanism is illustrated in Figure 3.

3.3. Characterization of the Silver Nanoparticles

The formation of the silver nanoparticles (AgNPs) was initially indicated spectrophotometrically using a UV-Vis spectrophotometer and then determined by particle size analysis. The UV-Vis spectrum of the synthesized AgNP suspension exhibited an absorption band within the wavelength range of 400–500 nm, which is characteristic of the localized surface plasmon resonance (LSPR) of

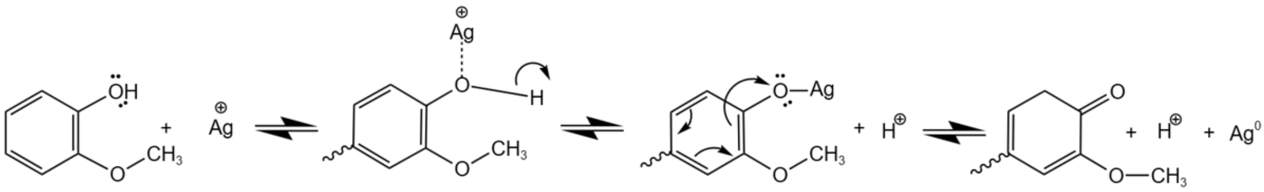

Figure 3. Mechanism of AgNPs formation by flavonoids [30].

Table 1. Phytochemical test results.

Test type	Photo Result	Result
Alkaloid		(-)
Flavonoid		(+)
Saponin		(-)
Tanin		(+)
Terpenoid	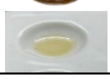	(+)

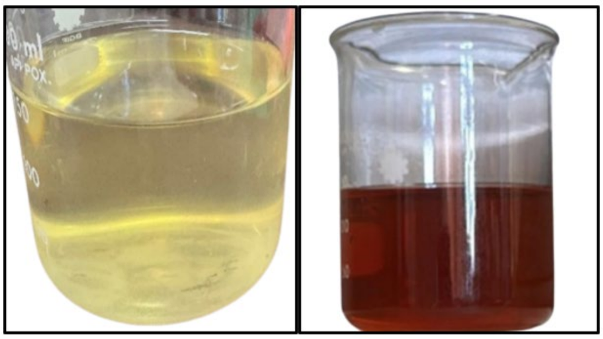

Figure 2. Changes in silver nanoparticle synthesis.

silver nanoparticles. The appearance of this absorption band confirms the formation of AgNPs due to the collective oscillation of conduction electrons on the nanoparticle surface upon interaction with incident light. The increase in absorption intensity with reaction time suggests the progressive formation and stabilization of AgNPs. Since the synthesized AgNPs were used directly without separation from the residual plant extract, the observed optical response may also include contributions from extract-derived surface species and capping molecules. Therefore, the UV-Vis results were interpreted primarily based on plasmonic absorption behavior rather than optical band-to-band transitions [31]. Figure 4 displays the spectra of the AgNPs after 1, 3, 23, 25, and 27 hours of cessation of the synthesis reaction. The spectra reveal a distinctive absorption peak in the range of 453.50 to 459.50 nm, indicating the formation of AgNPs through the Surface Plasmon Resonance (SPR) phenomenon, consistent with the characteristics of nanoparticles explained by Singh *et al.* [31]. The stability of the maximum wavelength and absorbance between the 23rd and 27th hours indicate that the synthesis reaction is approaching a steady state, with a decreasing rate of particle formation. Furthermore, the absence of a significant shift or drastic peak broadening indicates that the resulting particles are quite stable and do not experience excessive agglomeration. The UV-Vis spectrum of the synthesized AgNP suspension exhibited the characteristic localized surface plasmon resonance absorption associated with AgNP formation. Since the optical response is predominantly governed by plasmonic behavior and the available spectral range does not fully capture the absorption edge region required for Tauc analysis, optical bandgap estimation was not performed.

The Raman spectrum of the AgNP catalyst as shown in Figure 5 exhibited a broad band at around 3150–3200 cm^{-1}, which is attributed to O-H stretching vibrations, indicating the presence of surface hydroxyl groups and/or adsorbed moisture [32]. The bands observed in the region between 1100-1550 cm^{-1} are attributed to vibrational modes of surface-bound organic functional groups, including C-O, C-N, and C=C stretching vibrations [33]. The presence of these bands suggests that organic molecules are adsorbed on the AgNP surface and may function as capping or stabilizing agents, thereby contributing to nanoparticle stability and

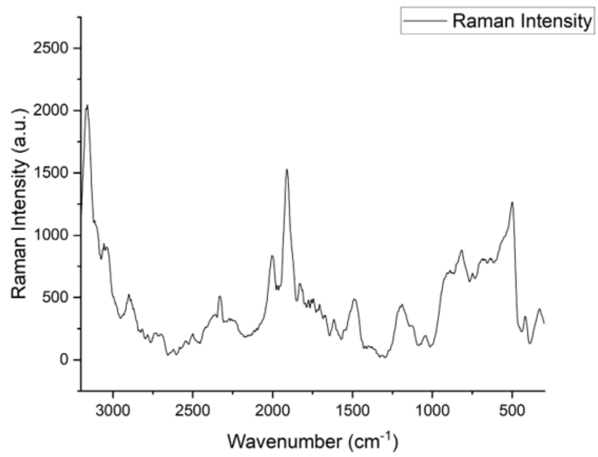

Figure 5. Raman spectroscopy of AgNP catalyst.

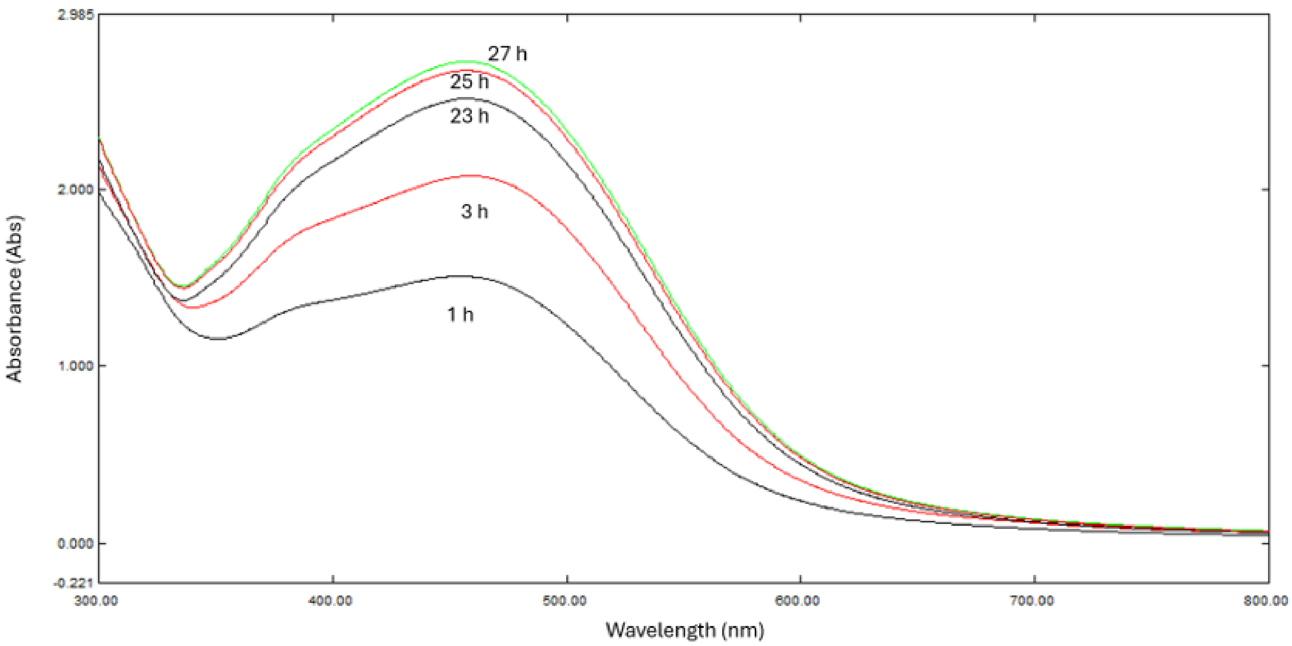

Figure 4. The visible spectra of AgNPs synthesised under varied synthesis time.

preventing aggregation [34]. Furthermore, the low-wavenumber bands within 500-900 cm^{-1} are attributed to Ag-O vibrations and metal-ligand interactions, indicating the interaction of silver nanoparticles with oxygen-containing functional groups on the catalyst surface [35]. These findings suggest the successful formation of AgNPs and support the presence of surface functionalization and metal-oxygen interactions that contribute to catalyst stability.

3.4. Particle Size Analysis

Particle size analysis was performed using PSA with the DLS method, which measures the scattering of infrared light due to the Brownian motion of particles in a liquid. The results of PSA measurements on nanoparticles showed an average particle size of 63.11 nm with a zeta potential of -18.14 mV and a Polydispersity Index (PI) of 0.2964. The results reveal a silver nanoparticle size of 63.11 nm, consistent with the characteristics of nanoparticles, which range from 1 to 100 nm. Homogeneous silver particle size is indicated by a Polydispersity Index (PI) below 0.5 indicate a relatively narrow particle size distribution and reduced heterogeneity of nanoparticles, while lower values (<0.3) suggest highly uniform particles [36] . The nanoparticle stability was measured by zeta potential, which was -18.14 mV. According to Liu *et al.* [37], a zeta potential value below -20mV indicates less colloidal stability, so that particles tend to interact with each other and form agglomerates. Nevertheless, the UV-Vis spectra in Figure 4 show that the particles do not undergo agglomeration, shown by the stable maximum wavelength for 27 hours, may be longer.

3.5. The Textile Waste Characteristics

Textile waste samples were obtained from a dyeing factory located in Banjar Akta, Gianyar. The waste appears very dark, with a jet-black color, qualitatively indicating a high content of organic dyes or complex compounds. The waste also has a distinctive odor resembling detergent, suspected to be due to residual surfactants and dyeing chemicals. Furthermore, the waste appears opaque, as evidenced by the absence of light penetration. The appearance of the waste can be seen in Figure 6.

Figure 6. Textile liquid waste.

Initial pH measurements of the wastewater yielded a pH of 7.26, indicating that the wastewater sample met the waste quality standards. Furthermore, the waste has high BOD and COD values of 181.944 mg/L and 333.015 mg/L, respectively. These results exceeded the quality standards stipulated in the Minister of Environment and Forestry Regulation No. 16 of 2019 concerning Wastewater Quality Standards for the Textile Industry.

3.6. The Textile Wastewater Degradation Optimization

The proposed photocatalytic degradation mechanism is based on the experimental observations obtained in the present study and supported by previous literature reports [5]. Under light irradiation, the AgNP catalyst may generate electron–hole pairs that subsequently participate in the formation of reactive oxygen species (ROS), including hydroxyl radicals ($\cdot OH$) and superoxide radicals ($O_2\cdot^-$), which are considered responsible for the degradation of contaminants. Similar ROS-mediated degradation pathways have previously been reported for AgNP-based photocatalytic systems, including dye degradation studies. However, radical scavenging experiments were not performed in the present work; therefore, the involvement of specific ROS species in the wastewater degradation process could not be directly confirmed, and the proposed mechanism should be considered as a plausible pathway. A detailed kinetic analysis was not performed due to the absence of time-dependent concentration data required for reliable reaction-order determination.

The degradation percentage of the waste under the varied pH is displayed in Figure 7. The graph in Figure 7 shows that the degradation decreases from pH of 2 to 6 and then increases gradually as the pH of the system increases. The degradation percentage reaches the highest (34.35%) at the highest pH tested, i.e.13. The reason for this result may be because under alkaline conditions, the surface of nanoparticles tends to become negatively charged due to deprotonation, which can influence the adsorption of reactants and increase the availability of hydroxide ions (OH^-). These conditions favour the generation of hydroxyl radicals ($\cdot OH$), the primary oxidizing species in photodegradation, thereby enhancing the degradation of organic molecules, including synthetic dyes [38,39]. This alkaline condition represents the operational conditions during the photodegradation process and does not represent the final condition of the wastewater. After the degradation process, the pH decreases approaching neutral, thus avoiding increasing environmental risks.

Figure 8 shows the photodegradation results of textile wastewater using various volumes of silver nanoparticles (AgNPs). The highest degradation (3.06%) was achieved with a AgNPs volume of 0.5 mL. A volume of 0.5 mL provides a balance between catalyst amount, active surface area, and light penetration, thus optimally supporting the formation of $\cdot OH$ and $\cdot O_2^-$ radicals for dye degradation [40]. The decrease in the degradation percentage at volumes above 0.5 mL is thought to be due to increased turbidity and shadowing effects that inhibit light penetration, resulting in uneven catalyst activation.

For the optimum duration of irradiation, it was found that the highest degradation percentage of the textile wastewater was achieved at 19.52% at 15 minutes (Figure 9). The longer the irradiation time, the AgNPs catalyst's ability to degrade dyes decreased. This can be seen at 90 minutes of irradiation, where the degradation percentage was only 7.74%. Therefore, the optimum degradation time is 15 minutes, a surprisingly short time, the shortest irradiation time ever reported which is promising for efficient waste treatment.

Table 2. Results of photodegradation percentage measurement.

Sample	%D dye	%D BOD	%D COD
A	34.27±0.01	5.54	9.10
B	37.44±0.007	11.08	12.22
C	37.76±0.02	5.54	8.66

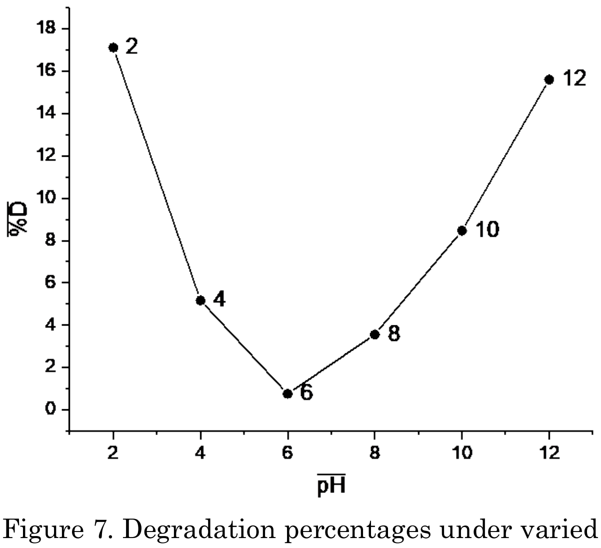

Figure 7. Degradation percentages under varied pH.

3.7. The Effectiveness of the Textile Waste Photodegradation

The effectiveness of the waste photodegradation was evaluated using three main parameters: the percentage of dye degradation, the reduction in Biochemical Oxygen Demand (BOD), and the Chemical Oxygen Demand (COD), which collectively reflect the degree of removal of the organic compounds in the waste. The evaluation results are shown in Table 2.

Based on the research results, the photodegradation effectiveness of textile dye waste using silver nanoparticles from soursop leaf extract (AgNPs) reached 34.27–37.76%, with a reduction in COD values of 8.66–12.22% and BOD of 5.54–11.08%. These results can be attributed to several important factors, including the physicochemical characteristics of the nanoparticles used, the intensity of visible light,

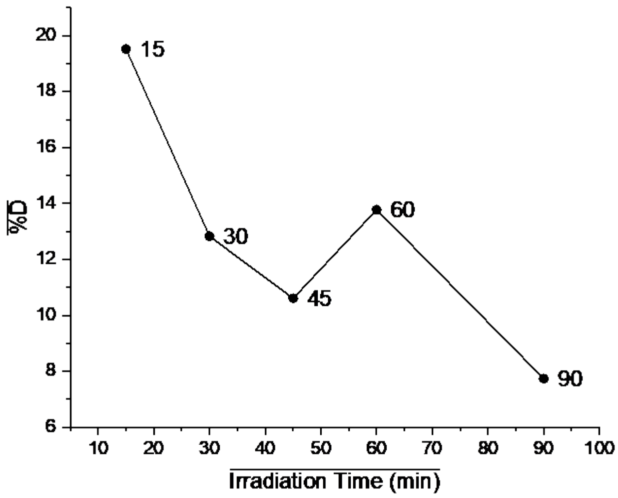

Figure 9. The corelation between the degradation percentages with irradiation times.

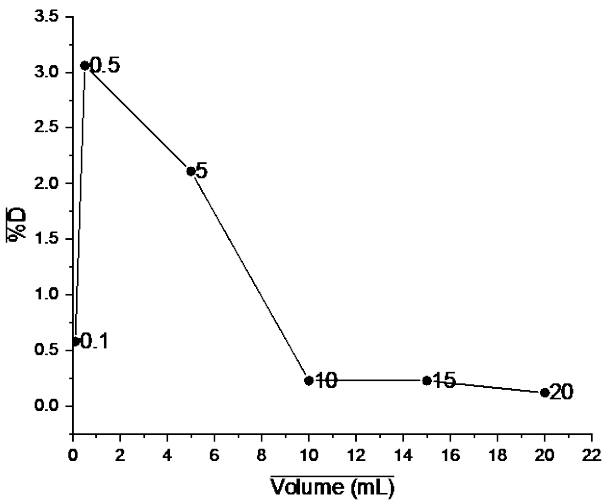

Figure 8. The changes in the degradation percentages with AgNP photocatalyst volumes.

and the initial wastewater conditions, such as the initial dye concentration and the presence of other interfering compounds.

Furthermore, the complex nature of the textile wastewater, containing various organic and inorganic compounds, and dyes with stable aromatic structures such as methylene blue or remazol, can hinder the degradation process. These structures require a large number of radicals to break down, and if the concentration of radicals generated is insufficient due to low photocatalyst efficiency, the photodegradation process is not optimal [41]. The low radiation penetration due to the dark and turbid wastewater is suspected to be responsible for lack of the radicals generated, thus a waste pretreatment to reduce the turbidity would improve the result.

Table 3 compares the photocatalytic performance of the present study with previously reported studies. Most reported studies investigated degradation of model dyes or synthetic wastewater under controlled conditions and achieved relatively high degradation efficiencies. In contrast, the present study evaluated the photocatalytic treatment of real textile wastewater, which contains a complex mixture of contaminants that may compete for active sites and reactive species during degradation. Furthermore, the present study is the most time effective offering fast waste treatment process. Therefore, although lower degradation efficiency was observed, the use of green-synthesized AgNPs for treatment of real wastewater represents a practical and environmentally relevant application.

This research has the advantages over other studies on textile waste photodegradation, both in terms of technical aspects, sample type, and application. One key advantage is the use of visible light as the energy source, allowing the process to proceed solely with sunlight, making it more energy-efficient and environmentally friendly, comparable to the work of Taymaz [43]. This selection was based on the compatibility of visible light photon energy with the band gap of silver nanoparticles (AgNPs), which ranges from 2–4 eV, allowing electron excitation without the aid of UV light. Another advantage is the use of real textile waste from the dyeing industry, rather than simulated dye solutions as commonly used in many studies. Real waste is much more complex because it contains many different chemicals, making its treatment more challenging but also more realistic for practical application.

Although the reduction in parameters namely BOD and COD was not optimal, this is understandable given the inherent complexity of the waste used. Therefore, this research provides an important foundation for further development. Overall, this research combines an innovative, realistic, and sustainable approach, making it relevant not only academically, but also for direct application in the waste processing industry in Indonesia.

4. Conclusion

Based on the results obtained, this study demonstrated that silver nanoparticles (AgNPs) synthesized using soursop leaf extract can function as a photocatalyst for textile wastewater photodegradation under visible-light irradiation. The optimum conditions were achieved at pH of 13, irradiation time of 15 min, and AgNP volume of 0.5 mL, resulting in degradation efficiencies of 34.37–37.76%, with reductions in BOD and COD of 5.54–11.08% and 8.66–12.22%, respectively. This study advances current knowledge by demonstrating the applicability of green-synthesized AgNPs for the treatment of actual textile wastewater rather than model dye systems, providing insight into their photocatalytic performance in more complex wastewater conditions.

Table 3. Comparative performance of photocatalysts for dye photodegradation.

Catalyst	Pollutant treated	Time (min)	%*D* dye	Reference
AgNPs (Visible)	Textile wastewater	15	34.27-37.76	Current Study
Fe–TiO_2 nanotube	Synthetic textile wastewater (Congo red + additives)	180	68-79.2	[42]
Ppy/ZnO@Co (Visible)	Cationic rhodamine B (RdB) and anionic direct yellow 50 (DY) dyes	45-70	97	[43]
$CoFe_2O_4$ (Visible light)	Congo red dye	120	97	[44]
CoFeCN (Visible Light)	Indigo Carmine dye	60	99.9	[45]

Acknowledgment

The authors would like to express their sincere gratitude to the Fundamental Research Grant Program (Hibah Penelitian Fundamental) of Universitas Udayana for the financial support provided for this research with the grant number B/324.98/UN14.4.A/PT.01.03/2026. The authors also acknowledge the facilities and academic support from Universitas Udayana that made this study possible.

CRedit Author Statement

Author Contributions: I. E. Suprihatin: Conceptualization, Investigation, Resources, Data Curation, Visualization, Supervision, Writing-Original Draft; A.A.S.A. Sukmaningsih: Investigation; N.M.U. Dwipayanti: Methodology; I.A.G. Widihati: Methodology; N.P. Diantariani: Writing- Review and editing; N.G.A.D.A. Suastuti: Investigation; I.G.A.K.S.P. Dewi: Investigation. All authors have read and agreed to the published version of the manuscript.

References

[1] Garg, A., Chopra, L. (2022). Materials Today : Proceedings Dye Waste : A significant environmental hazard. *Materials Today: Proceedings*, 48, 1310–1315. DOI: 10.1016/j.matpr.2021.09.003.

[2] Abdelhamid, A.E., Elsayed, A.E., Naguib, M., Abobakr, E. (2023). Effective Dye Removal by Acrylic - Based Membrane Constructed from Textile Fibers Waste. *Fibers and Polymers*, 24(7), 2391–2399. DOI: 10.1007/s12221-023-00247-z.

[3] Guo, W., Guo, T., Zhang, Y., Yin, L., Dai, Y. (2023). Chemosphere Progress on simultaneous photocatalytic degradation of pollutants and production of clean energy : A review. *Chemosphere*, 339(May), 139486. DOI: 10.1016/j.chemosphere.2023.139486.

[4] Farooque, M., Tuzen, M., Yar, M., Saleh, T.A. (2024). Trends in photocatalytic degradation of organic dye pollutants using nanoparticles : A review. *Inorganic Chemistry Communications*, 159(October 2023), 111613. DOI: 10.1016/j.inoche.2023.111613.

[5] Suprihatin, I.E., Widihati, I.A.G., Suastuti, N.G.A.D.A., Lestari, G.A.D., Diantariani, N.P., Khoiriah, K., Sukmaningsih, A.A.S.A. (2026). Eco-Friendly synthesis of silver nanoparticles using soursop leaf extract for photocatalytic degradation of congo red and Indigo Carmine dyes. *Nanotechnology for Environmental Engineering*, 11(27), 1–13. DOI: 10.1007/s41204-026-00518-z.

[6] Bai, X., Chen, W., Wang, B., Sun, T., Wu, B., Wang, Y. (2022). Photocatalytic Degradation of Some Typical Antibiotics : Recent Advances and Future Outlooks. *International Journal of Molecular Sciences*, 23(15), 8130. DOI: 10.3390/ijms23158130.

[7] Lee, D., Kim, M., Danish, M., Jo, W. (2023). State-of-the-art review on photocatalysis for efficient wastewater treatment : Attractive approach in photocatalyst design and parameters affecting the photocatalytic degradation. *Catalysis Communications*, 183(September), 106764. DOI: 10.1016/j.catcom.2023.106764.

[8] Bikerchalen, S., Akhsassi, B., Bakiz, B., Villain, S., Taoufyq, A., Guinneton, F. (2025). Photocatalytic degradation of Rhodamine B dye over oxygen-rich bismuth oxychloride Bi 24 O 31 Cl 10 photocatalyst under UV and Visible light irradiation : Pathways and mechanism. *Journal of Physics and Chemistry of Solids*, 196(July 2024) DOI: 10.1016/j.jpcs.2024.112342.

[9] Mozdbar, A., Nouralishahi, A., Fatemi, S., Sadat, F. (2023). The impact of Carbon Quantum Dots (CQDs) on the photocatalytic activity of TiO 2 under UV and visible light. *Journal of Water Process Engineering*, 51(January), 103465. DOI: 10.1016/j.jwpe.2022.103465.

[10] Mahmoud, M.A., Alsehli, B.R., Alotaibi, M.T., Hosni, M., Shahat, A. (2024). A comprehensive review on the application of semiconducting materials in the degradation of effluents and water splitting. *Environmental Science and Pollution Research*, 31, 3466–3494. DOI: 10.1007/s11356-023-31353-3.

[11] Gharibshahi, L., Saion, E., Gharibshahi, E., Shaari, A.H., Matori, K.A. (2017). Structural and Optical Properties of Ag Nanoparticles Synthesized by Thermal Treatment Method. *Materials*, 10(4), 1–13. DOI: 10.3390/ma10040402.

[12] Jin, Z., Xiao, S., Dong, H., Xiao, J., Tian, R., Chen, J. (2022). Adsorption and catalytic degradation of organic contaminants by biochar : Overlooked role of biochar's particle size. *Journal of Hazardous Materials*, 422(August 2021), 126928. DOI: 10.1016/j.jhazmat.2021.126928.

[13] Sohail, M., Ramzan, N., Najam, T., Abbas, G., Gu, X. (2022). Science of the Total Environment Metallic nanoparticles for catalytic reduction of toxic hexavalent chromium from aqueous medium : A state-of-the-art review. *Science of the Total Environment*, 829, 154475. DOI: 10.1016/j.scitotenv.2022.154475.

[14] Franco, D., Calabrese, G., Pietro, S., Guglielmino, P., Conoci, S. (2022). Metal-Based Nanoparticles : Antibacterial Mechanisms and Biomedical Application. *Microorganism*, 10(9), 1778. DOI: 10.3390/microorganisms10091778.

[15] Elbadawy, H.A., Elhusseiny, A.F., Hussein, S.M., Sadik, W.A. (2023). Sustainable and energy-efficient photocatalytic degradation of textile dye assisted by ecofriendly synthesized silver nanoparticles. *Scientific Reports*, 13(1), 1–13. DOI: 10.1038/s41598-023-29507-x.

[16] Shahzadi, S., Fatima, S., Shafiq, Z., Ramzan, M., Ashraf, S. (2025). A review on green synthesis of silver nanoparticles (SNPs) using plant extracts : a multifaceted approach in photocatalysis , environmental. *RSC Advances*, 15, 3858–3903. DOI: 10.1039/d4ra07519f.

[17] Saravanan, A., Kumar, P.S., Karishma, S., Vo, D.N., Jeevanantham, S., Yaashikaa, P.R., Susan, C. (2021). Chemosphere A review on biosynthesis of metal nanoparticles and its environmental applications. *Chemosphere*, 264, 128580. DOI: 10.1016/j.chemosphere.2020.128580.

[18] Co, O., Lithi, I.J., Ahmed, I., Sarwaruddin, A.M. (2025). A review on the green synthesis of metal (Ag, Cu). *Nanoscale Advances*, 7, 2446–2473. DOI: 10.1039/d5na00037h.

[19] Oghenewogaga, J., Efeoghene, A., Essaghah, A., Umar, H., Ahmed, D.S., Alamiery, A.A. (2025). Eco-friendly nanoparticle phytosynthesis via plant extracts_ Mechanistic insights, recent advances, and multifaceted uses. *Nano TransMed*, 4 (March), 100080. DOI: 10.1016/j.ntm.2025.100080.

[20] Husen, A., Siddiqi, K.S. (2014). Phytosynthesis of nanoparticles : concept , controversy and application. *Nanoscale Research Letters*, 9(1), 1–24. DOI: 10.1186/1556-276X-9-229.

[21] Duy, N., Minh, N., Minh, L., Tan, L. (2022). Colloids and Surfaces B : Biointerfaces Phytosynthesis of silver nanoparticles using Mangifera indica leaves extract at room temperature : Formation mechanism , catalytic reduction, colorimetric sensing , and antimicrobial activity. *Colloids and Surfaces B: Biointerfaces*, 220 (September), 112974. DOI: 10.1016/j.colsurfb.2022.112974.

[22] Osarumwense, O., Anthony, I., Idowu, T., Toluwabori, S. (2025). Soursop (Annona muricata) Nutritional Composition, Bioactivities and its Potential Applications : A Review. *Waste and Biomass Valorization*. 17, 3651–3665. DOI: 10.1007/s12649-025-03282-4

[23] Santos, I.L., Manoel, A., Amante, E.R., Helena, L. (2023). Soursop (Annona muricata) Properties and Perspectives for Integral Valorization. *Foods*, 12, 1448. DOI: 10.3390/foods12071448.

[24] Mutakin, M., Fauziati, R., Fadhilah, F.N., Zuhrotun, A., Amalia, R., Hadisaputri, Y.E. (2022). Pharmacological Activities of Soursop (Annona muricata Lin.). *Molecules*, 27, 1–17. DOI: 10.3390/molecules27041201.

[25] Lestari, G.A.D., Suprihatin, I.E., Sibarani, J. (2019). Sintesis Nanopartikel Perak (NPAg) Menggunakan Ekstrak Air Buah Andaliman (Zanthoxylum acanthopodium DC.) dan Aplikasinya pada Fotodegradasi Indigosol Blue. *Jurnal Kimia Sains dan Aplikasi*, 22(5), 200–205. DOI: 10.14710/jksa.22.5.200-205.

[26] Gao, Y., Sun, W., Yang, W. et al. (2017) Creation of Pd/Al2O3 Catalyst by a Spray Process for Fixed Bed Reactors and Its Effective Removal of Aqueous Bromate. *Sci. Rep*. 7, 41797. DOI: 10.1038/srep41797.

[27] Mirzaeifard, Z., Shariatinia, Z. (2024). Economical, one-pot, and green synthesis of plant-based carbon quantum dots for efficient visible-light photocatalytic dye degradation and water purification. *Journal of the Taiwan Institute of Chemical Engineers*, 163(June), 105655. DOI: 10.1016/j.jtice.2024.105655.

[28] Hernandez-fuentes, G.A., Delgado-enciso, O.G., Larios-cedeño, E.G., Juan, M.S., Ceballos-magaña, S.G., Pineda-urbina, K., Alcal, M.A., Magaña-vergara, N.E., Delgado-enciso, J., Uriel, D., Diaz-martinez, J., Garza-veloz, I., Martinez-fierro, M.L., Rodriguez-sanchez, I.P., Delgado-enciso, I. (2024). Comparative Analysis of Infusions and Ethanolic Extracts of Annona muricata Leaves from Colima , Mexico : Phytochemical Profile and Antioxidant Activity. *Life*, 14(12), 1–23. DOI: 10.3390/life14121702.

[29] Zuhrotun, A., Oktaviani, D.J., Hasanah, A.N. (2023). Biosynthesis of Gold and Silver Nanoparticles Using Phytochemical Compounds. *Molecules*, 23(7), 3840. DOI: 10.3390/molecules28073240.

[30] Fajri, N., Putri, L.F.A., Prasetio, M.R., Azizah, N., Pratama, Y., Susanto, N.C.A. (2022). Potensi batang pisang (Musaparadisiacal) sebagai bioreduktor dalam green sintesis Ag nanopartikel. *Jurnal Penelitian Sains*, 24(1), 33–37. DOI: 10.56064/jps.v24i1.668.

[31] Singh, T.D., Singh, T.G., Henam, S.D. (2017). Green synthesis, growth and catalytic activity of silver nanoparticles. *Green Materials*, 5(4) DOI: 10.1680/jgrma.17.00022.

[32] Mohaček-Grošev, V., Furić, K., Vujnović, V. (2022). Raman study of water deposited in solid argon matrix. *Spectrochimica Acta - Part A: Molecular and Biomolecular Spectroscopy*, 269 DOI: 10.1016/j.saa.2021.120770.

[33] Kora, A.J., Arunachalam, J. (2012). Green fabrication of silver nanoparticles by gum tragacanth (astragalus gummifer): A dual functional reductant and stabilizer. *Journal of Nanomaterials*, 2012 DOI: 10.1155/2012/869765.

[34] Wonner, K., Murke, S., Alfarano, S.R., Hosseini, P., Havenith, M., Tschulik, K. (2022). Operando electrochemical SERS monitors nanoparticle reactions by capping agent fingerprints. *Nano Research*, 15(5), 4517–4524. DOI: 10.1007/s12274-021-3999-2.

[35] Tang, Z., Chen, T., Liu, K., Du, H., Podkolzin, S.G. (2021). Atomic, Molecular and Hybrid Oxygen Structures on Silver. *Langmuir*, 37(39), 11603–11610. DOI: 10.1021/acs.langmuir.1c01941.

[36] Farkas, N., Kramar, J.A. (2021). Dynamic light scattering distributions by any means. *Journal of Nanoparticle Research*, 23(5) DOI: 10.1007/s11051-021-05220-6.

[37] Liu, J., Fan, Y., Sun, Y., Wang, Z., Zhao, D., Li, T., Dong, B., Tang, C.Y. (2021). Modelling the critical roles of zeta potential and contact angle on colloidal fouling with a coupled XDLVO - collision attachment approach. *Journal of Membrane Science*, 623 (November 2020), 119048. DOI: 10.1016/j.memsci.2021.119048.

[38] Arellano-Cortaza, M., Ramirez-Moralez, E., Pal, U., Perez-Hernandez, G., Rojas-blanco, L. (2021). pH dependent morphology and texture evolution of ZnO nanoparticles fabricated by microwave-assisted chemical synthesis and their photocatalytic dye degradation activities. *Ceramics International*, 47, 27469–27478. DOI: 10.1016/j.ceramint.2021.06.170.

[39] Su, S., Siretanu, I., Ende, D. Van Den, Mei, B., Mul, G., Mugele, F. (2021). Facet-Dependent Surface Charge and Hydration of Semiconducting Nanoparticles at Variable pH. *Advanced Materials*, 33, 1–8. DOI: 10.1002/adma.202106229.

[40] Tam, K.T., Ngan, N.T.K. (2022). Green synthesis of silver nanoparticles using citrus maxima peel extract for photocatalytic degradation of methylene blue , and rhodamine b under sunlight. *TNU Journal of Science and Technology*, 227(08), 410–416. DOI: 10.34238/tnu-jst.5896.

[41] Bahadori, E., Rapf, M., Di, A., Rossetti, I. (2020). Photochemical vs photocatalytic azo-dye removal in a pilot free-surface reactor : Is the catalyst effective ? *Separation and Purification Technology*, 237 (July 2019), 116320. DOI: 10.1016/j.seppur.2019.116320.

[42] Zafar, Z., Fatima, R., Kim, J.O. (2021). Experimental studies on water matrix and influence of textile effluents on photocatalytic degradation of organic wastewater using Fe–TiO2 nanotubes: Towards commercial application. *Environmental Research*, 197(March), 111120. DOI: 10.1016/j.envres.2021.111120.

[43] Taymaz, B.H. (2023). A novel Ppy / ZnO @ Co ternary nanocomposite with enhanced visible light-driven photocatalytic performance. *Journal of the Taiwan Institute of Chemical Engineers*, 144, 104741. DOI: 10.1016/j.jtice.2023.104741.

[44] Magdalane, C.M., Priyadharsini, G.M.A., Kaviyarasu, K., Jothi, A.I., Simiyon, G.G. (2021). Synthesis and characterization of TiO2 doped cobalt ferrite nanoparticles via microwave method: Investigation of photocatalytic performance of congo red degradation dye. *Surfaces and Interfaces*, 25(June), 101296. DOI: 10.1016/j.surfin.2021.101296.

[45] Aldaghri, O. (2025). Efficient photocatalytic degradation of indigo carmine dye by CoFe2O4@g-C3N4 nanocomposite. *Journal of Science: Advanced Materials and Devices*, 10(4), 100988. DOI: 10.1016/j.jsamd.2025.100988.